Analysis Note: $\psi' \to \pi^+\pi^- J/\psi$, $J/\psi \to l^+l^-$ and $B(J/\psi \to l^+l^-)$

F. A. Harris
Department of Physics and Astronomy
The University of Hawaii
2505 Correa Road
Honolulu, HI 96822
USA

Introduction

The $\psi' \to \pi^+\pi^- J/\psi$, $J/\psi \to l^+l^-$ sample is extremely important. As mentioned previously [1], it is used to determine the line shape of the J/ψ peak in the m_{recoil} distribution in the determination of the number of ψ' events. More importantly, this sample can be used to determine the J/ψ leptonic branching ratios, as well as to study the physics of the $\psi' \to \pi^+\pi^- J/\psi$ process. The branching ratio $B(J/\psi \to ll) \simeq 6.0$ %.

This informal analysis note describes event selection, background checks, agreement with the Monte Carlo, and the determination of $B(J/\psi \to l^+l^-)$. The study of the physics of the $\psi' \to \pi^+\pi^- J/\psi$ process is covered in a separate note.

Lepton ID

In order to select clean $\psi' \to \pi^+\pi^- J/\psi$, $J/\psi \to l^+l^-$ events, it is necessary to require PID for the leptons, as well as to make kinematic cuts. In the following, we use the new dE/dx and TOF routines of Li Xinhua and Bill Dunwoodie[2].

Fig. 1 shows Xse of one track versus Xse of the other track. Xse is the corrected Xs value assuming the electron hypothesis. We get nice separation of ee events from other events using ONLY dE/dx information, so we will make use of both the drift chamber and the shower counter to identify electrons. This is very useful because Sober does not model the rib region of the shower counter well and gives an underestimate of the electron identification efficiency. In addition, having two independent systems allows us to make comparisons between them to determine the efficiency and background of each. We can use data to determine the PID efficiency!

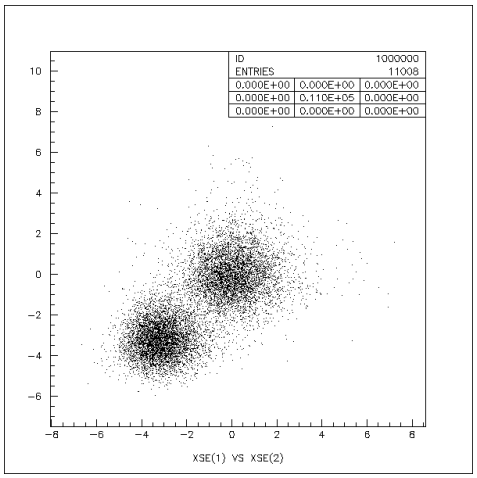

Figure 1: Xse of track 1 versus Xse of track 2, where Xse is calculated assuming that tracks are electrons. Events are $\pi^+\pi^-\mu^+\mu^-$ and $\pi^+\pi^-e^+e^-$ events from the '95 data. The round cluster at (0,0) is due to the e^+e^- events, while the cluster at approximately (-3,-3) is due to the $\mu\mu$ events.

Momentum Dependence of PID

Figs. 2A and 2B show the energy deposited in the shower counter (E) versus momentum (p) for tracks not in the rib region. Electron and muon events are well separated at high momentum. Figs. 2C and 2D show E/p versus p for the same tracks. Again electron and muon events are well separated at high momentum. The separation is poorer at lower momentum. Muon events are flat in E versus p, while electron events are flat in E/p versus p.

Fig. 3 shows Xse versus the momentum. In Fig. 3A, there are clear kaon, proton, and pion bands. Fig. 3B shows where electrons and muons occur on the plot. Clearly there are regions in momentum where protons and electrons overlap and where kaons and electrons overlap in Xse.

ee Selection

We use the following algorithm:

- Define the rib region of the shower counter: $|zsh| < 0.04$m or $0.8 < |zsh| < 1.0$m.
- If both tracks are outside of the rib region and have momenta > 0.8 GeV/c, use the shower counter to define electrons and cut on E/p of track 1 versus E/p of track 2.
- Otherwise, use the drift chamber and cut on Xse of track 1 versus Xse of track 2. Also require $E/p > 0.5$ if one of the tracks is outside the rib region.

The cut is made on z at the shower counter rather than $\cos\theta$ because the resolution is better. The $\cos\theta$ distribution is smeared out because of the z extent of the interaction region.

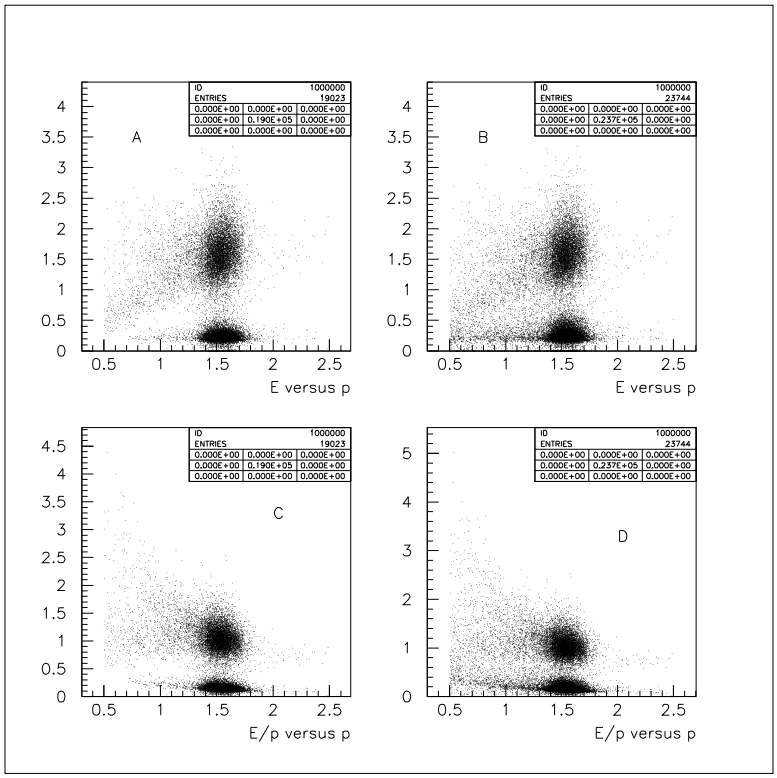

Figure 2: Shower counter energy (E) response versus momentum (p) for $\pi^+\pi^- l^+ l^-$ events using '95 data. A.) E versus p for events with identified leptons; B.) E versus p for events without lepton identification required; C.) E/p versus p with identified leptons; D.) E/p versus p for events without lepton identification required . Most tracks occur at 1.5 GeV/c. The separation at high momentum is very good; it is less so at low momentum.

Figure 3: Xse versus p for $\pi\pi l^+ l^-$ events from the '95 data. A.) Events without identified electrons or muons. Bands due to π's, K's, and protons are clearly visible. B.) Electron and muon events. The upper cluster contains the electron events. Note that electron events overlap proton events at about 1.2 GeV/c and K's at about 0.5 GeV/c.

ee PID Efficiency and Background

Since we have good separation of electrons from other particles in both the drift chamber and the shower counter, we can determine the electron identification efficiency and the background by comparing one system with the other. In Fig. 4, the distribution of E/p of one track versus the E/p of the other is shown for events selected on the basis of Xse of one track versus the Xse of the other for events with neither track in the rib region and with $p > 0.8$ GeV for the '95 data. Most events occur in a cluster centered at (1,1), but there are a few background events located near the origin. By counting the number of background events at the origin, it is possible to determine the Xse vs. Xse cut background rate. By determining how many events in the cluster at (1,1) pass the E/p versus E/p cut, we can determine the efficiency (ϵ_{EP}) of this cut.

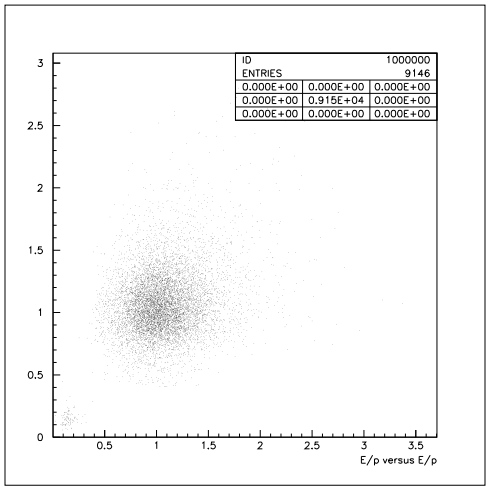

Figure 4: Distribution of E/p for track 1 versus E/p of track 2 for $\pi^+\pi^-e^+e^-$ events outside of the rib region and selected using cuts on Xse of track 1 versus Xse of track 2 for the '95 data. Events near the origin are used to calculate the background associated with the Xse versus Xse cut. Determining how many events in the cluster at (1,1) are inside the E/p versus E/p cut region gives the efficiency of this cut (ϵ_{EP}).

Fig. 5 shows the Xse of one track versus the Xse of the other for events selected on the basis of the E/p versus E/p cut for events with neither track in the rib region in the '95 data. Only a few events occur in the non-electron region (compare this figure with Fig. 1). These are used to determine the background rate associated with the E/p versus E/p cut (ϵ_{Xse}). Determining how many of the electron cluster events pass the Xse versus Xse cut determines the efficiency of this cut.

For events with neither track in a rib region and with both tracks having $p > 0.8$ GeV, ee events are identified using the shower counter with the E/p cuts:

1. $(E/p)_1 > (E/p)_{1cut}$ and $(E/p)_2 > 1$ –OR–
2. $(E/p)_2 > (E/p)_{2cut}$ and $(E/p)_1 > 1$ –OR–

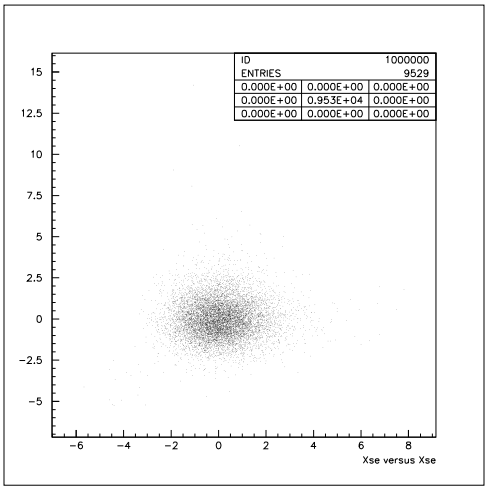

Figure 5: Distribution of Xse for track 1 versus Xse of track 2 for $\pi^+\pi^-e^+e^-$ events outside of the rib region and selected using cuts on E/p of track 1 versus E/p of track 2. Events below the origin and to the left are used to calculate the background associated with the E/p versus E/p cut. Determining how many events are inside the Xse versus Xse cut region gives the efficiency of this cut (ϵ_{Xse}).

3. $(E/p)_r = \sqrt{[(E/p)_1 - 1]^2 + [(E/p)_2 - 1]^2}$ is inside an ellipse formed using $(E/p)_{1cut}$ and $(E/p)_{2cut}$.

The $(E/p)_{cut}$ value depends on p and is given by $(E/p)_{cut} = 0.6/p$.

A complication arises because the E/p distribution of simulated events looks rather different than the E/p distribution of real events. To insure that the correct efficiency is determined when cutting on Monte Carlo events, we shift and scale the Monte Carlo E/p distribution using shifts and scale factors determined by Program MnFit [3]. Fig. 6 shows the E/p distributions for '93 data, for Monte Carlo data, and for shifted and scaled Monte Carlo data.

For events with a track in the rib region or with $p < 0.8$ Gev/c, ee events are identified using the drift chamber with the following cuts:

1. $\sqrt{\frac{Xse(1)^2}{\sigma(1)} + \frac{Xse(2)^2}{\sigma(2)}} < 2.0$ –OR–

2. If $Xse(1) > 1.0$ or $Xse(2) > 1.0$, $\sqrt{\frac{Xse(1)^2}{\sigma(1)} + \frac{Xse(2)^2}{\sigma(2)}} < 3.0$.

3. If one track is not in the ribs, E/p of that track must be > 0.5.

For the Xse versus Xse cut, a routine similar to OKXSPI[4] is used. For each data set ('93, '95, 93' Monte Carlo, and 95' Monte Carlo), the mean and two sigmas of a bifurcated Gaussian are determined. All cuts are made in terms of the sigmas (plus side or minus side) for that distribution. This is necessary since the Monte Carlo does not simulate the data well.

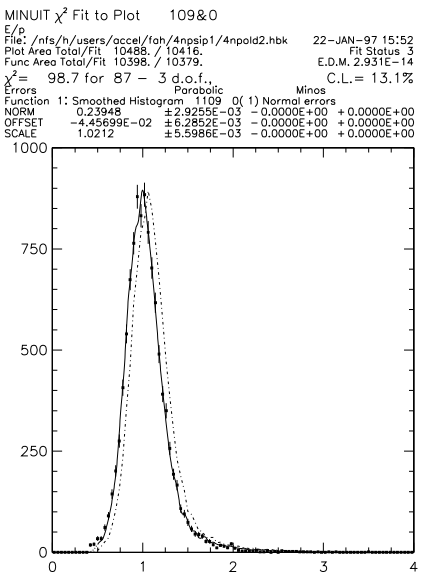

Figure 6: E/p distributions for '93 data (points with error bars), Monte Carlo data (dash-dot curve), and shifted and scaled Monte Carlo data (solid curve). The latter shows good agreement with the '93 data.

Efficiency and Background Results using our final selection cuts (see below) are shown in Table 1 for the '93 data and Table 2 for the '95 data. Fig. 7 shows the z distribution of the electron events. The distribution is quite smooth through the rib regions.

Table 1: Efficiencies and Backgrounds of ee Identification Schemes for '93 Data for the final cuts. Overall is determined by weighting according to the percentage of events obtained with the two selection methods.

Method	Background (%)	Efficiency (%)	MC Eff (%)
E/p vs E/p	0.0	98.3	98.7
Xse vs Xse	0.3	94.1	93.6
Overall	0.1	97.1	97.3

Table 2: Efficiencies and Backgrounds of ee Identification Schemes for '95 Data for the final cuts. Overall is determined by weighting according to the percentage of events obtained with the two selection methods.

Method	Background (%)	Efficiency (%)	MC Eff (%)
E/p vs E/p	0.0	96.8	98.4
Xse vs Xse	0.34	95.0	93.4
Overall	0.1	96.3	97.0

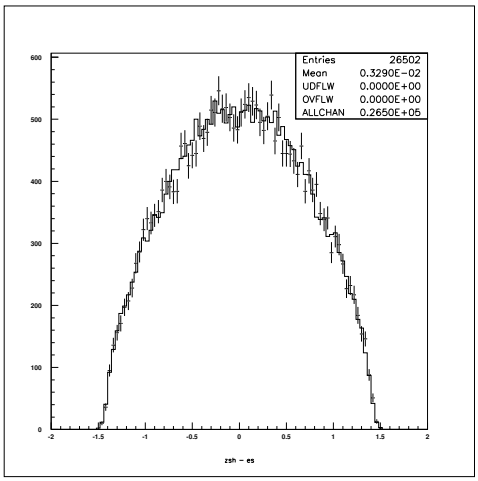

Figure 7: Distribution of the z coordinate at the shower counter for identified electron in $\psi' \to \pi^+\pi^- J/\psi$, $J/\psi \to e^+e^-$ events. Dots with error bars are data and the histgram is Monte Carlo data. The distributions are smooth through the rib regions.

Muon Id

Here we only have one PID system to identify high energy muons so it is not possible to use the events themselves to determine the muon PID efficiency and background as in the electron case. Tracks are defined to be muons if they are found to have 2 good hits in the muon system as defined by the routine MYMUID [5]. Muon events can be defined requiring either 1 or 2 muon tracks. More events are obtained and better agreement between $B(ee)$ and $B(\mu\mu)$ is obtained if we allow both 2μ and 1μ track events. For 1μ events, an additional requirement $|(m_{\mu\mu} - m_{J/\psi})| < 0.25 GeV/c^2$ is made to reduce background. Fig. 8 shows the invariant mass distribution ($m_{\mu\mu}$) of the events with only one identified muon track. This distribution has been fit using the signal shape of the two muon track events plus a polynomial background. The background under the data within the cut region is small, about 4% of the 1 muon track events in the cut region or less than 1% of total sample of 1-μ and 2-μ track events. The 1-μ events make up about 22% of the $\mu\mu$ event sample.

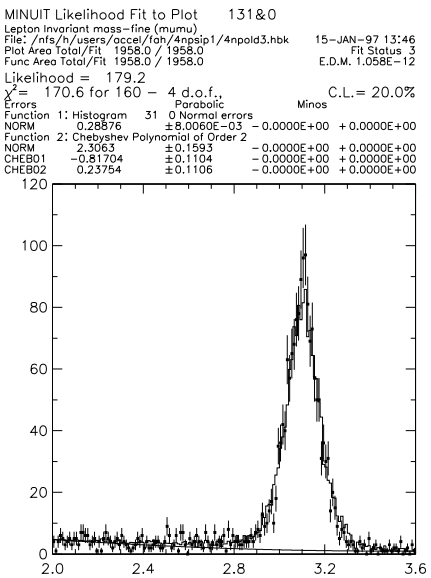

Figure 8: Invariant mass distribution of $\pi^+\pi^-\mu^+\mu^-$ events with only one muon track identified by the muon system. Data (points with error bars) are fit with signal (from events with both muons identified by the muon system and background (2nd order). Background in cut region between 2.85 and 3.35 GeV/c^2 is small.

Event Selection

Most $\psi' \to \pi^+\pi^- J/\psi$, $J/\psi \to l^+l^-$ events occur in the 4 prong sample, however a significant contribution is found in the > 4 prong sample. We will begin by describing the 4 prong selection.

Pion Cuts:

The pion cuts are the same as in the "Analysis Note on the Number of ψ''s" but are given again for convenience.

- good run (PPRUNS: status > 0 or 1).
- mnfit = 2, -9, -19.
- $|\cos\theta| < 0.8$ for π's
- $p_\pi < 0.5 GeV/c$
- $pxy(\pi) > 0.1 GeV/c$
- $\Sigma Hit_\pi^{dE/dx} > 13$. $\Sigma Hit_\pi^{dE/dx}$ is the number of hits used in the dE/dx calculation.
- $|\chi_\pi^{dE/dx}| < 3.0$. $\chi_\pi^{dE/dx} = \frac{(dE/dx)_{meas} - (dE/dx)_{exp}}{\sigma}$.
- $m_{\pi\pi} > 0.35 GeV/c^2$ to eliminate gamma conversions.
- $3.0 < m_{recoil} < 3.2 GeV/c^2$

Initial Lepton Cuts

- Events must satisfy PID requirements described in the previous section.
- $0.5 < p_l < 2.5 GeV/c$
- $|\cos\theta| < 0.75$ for electrons, < 0.65 for muons.

With these cuts, there is still background in the electron sample. See Figs. 9 A-D. There are many more data events where both tracks have low momentum than there are for Monte Carlo events in the electron event samples. The muon events look much cleaner.

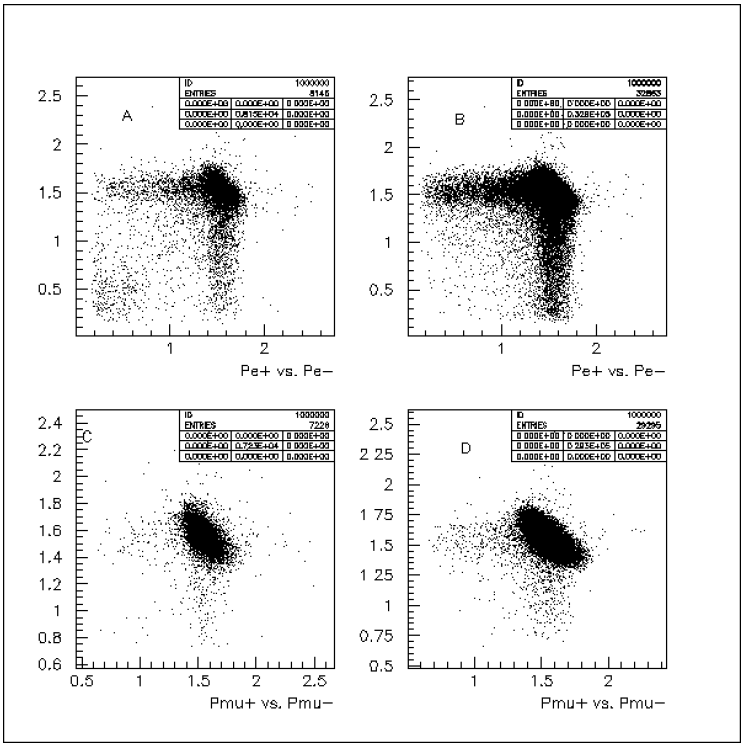

Figure 9: Plot of p_{l^+} versus p_{l^-} for $\psi' \rightarrow \pi^+\pi^- J/\psi$, $J/\psi \rightarrow l^+l^-$ events. A.) p_{e^+} vs p_{e^-} for $\pi^+\pi^- e^+e^-$ events. The cluster at low p is background. B.) p_{e^+} vs p_{e^-} for Monte Carlo $\pi^+\pi^- e^+e^-$ events. C.) p_{μ^+} vs p_{μ^-} for $\pi^+\pi^-\mu^+\mu^-$ events. D.) p_{μ^+} vs p_{μ^-} for Monte Carlo $\pi^+\pi^-\mu^+\mu^-$ events.

Additional Lepton Cuts

In order to reduce the background, we use additional kinematic cuts:

- $\cos\theta_{l^+l^-} < -0.85$. This is the cosine of the angle between the two leptons in the lab. See Fig. 10. The leptons from this decay are almost back to back.

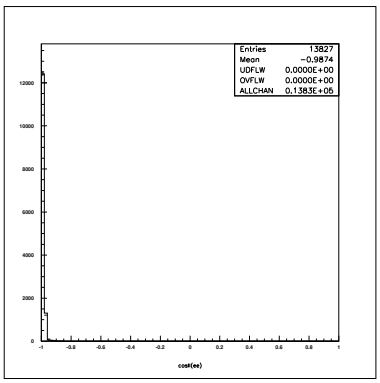

Figure 10: Cosine of the angle between the two leptons in $\pi^+\pi^-e^+e^-$ events ('95 data). Dots with error bars are data; histogram is Monte Carlo data.

- $\cos\theta^{cm}_{l^+l^-} < -0.975$. This is the cosine of the angle between the two leptons in the J/ψ CM. See Fig. 11. The leptons are even more back-to-back in the CM system.

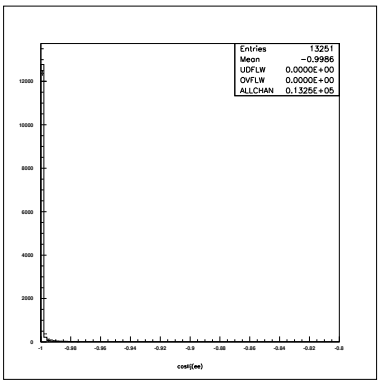

Figure 11: Cosine of the angle between the two leptons in $\pi^+\pi^-e^+e^-$ events ('95 data). Dots with error bars are data; histogram is Monte Carlo data.

- p_{l^+} or $p_{l^-} > 1.4 GeV/c$. This cut is used to cut out the background region (see Fig. 9A.)

Selection of > 4 Prong Events.

There is small but significant number of events in the > 4 prong sample. These events are primarily events where the hits on one track have been used to form two fitted tracks, which have nearly the same angles and momenta. Some of the track hits are used in one fitted track, and other hits are used in the other fitted track.

These events are potentially much more complicated than the 4 prong events, so in addition to the cuts mentioned above, the following cuts are made to simplify the analysis and to reduce background:

1. $2.2 > p_l > 1.0$ GeV/c.
2. $7 > NCHRG > 4$.
3. Only one good ee pair or $\mu\mu$ pair.
4. $|m_{l^+l^-} - m_{J/\psi}| < 0.25 GeV/c^2$.

The contribution of the > 4 prong events is indicated in Table 3.

Table 3: Contribution of > 4 prong events

Sample	$\mu\mu$ events (%)	ee events (%)
'93 data	3.4	3.3
'95 data	3.9	3.6

Hadronic Background Check.

It is important to test whether there are hadronic events getting into the $\psi' \to \pi^+\pi^- J/\psi, J/\psi \to l^+l^-$ events. To do this, we analyzed Daniela's $\rho\pi$ events from the '95 data.

Daniela's Cuts:

- ICODE > 0
- $1 < NNEU < 9$
- NCHRG $= 4$
- $\Sigma q_i = 0$
- $E_\gamma > 0.05$GeV
- $\cos\gamma < 0.96$
- $|\cos\theta| < 0.8$
- $\chi^2 < 20$ (4C fit)
- π^o mass cut: 50 MeV
- recoil mass against low momentum pair: (3.0 - 3.2 GeV/c^2)

- ρ cut: $0.6 < m(\pi\pi) < 0.95 GeV/c^2$

NOTE: Cuts to eliminate ee and $\mu\mu$ events were not used.

The events were analyzed thru the $\psi' \to \pi^+\pi^- J/\psi, J/\psi \to l^+l^-$ programs. The results are shown in Table .

Table 4: $N(\pi\pi\rho\pi)$ Results For '95 Data.

Cuts	Events
None	1350
π cuts and $\cos\theta_{l^+l^-}$ cut	471
Also Require lepton ID	21
Plus p_l cuts, and $\cos\theta^{cm}_{l^+l^-}$ cut	10

We can use these results to make a background estimate. Daniela obtains: $\epsilon(\pi\pi\rho\pi) = 0.12$. We assume $\epsilon(\pi^+\pi^-\pi^+\pi^-) \approx \epsilon(\pi\pi ll)$. Then

$$N_{BKG} = 10\frac{\epsilon(\pi\pi ll)}{\epsilon(\pi\pi\rho\pi)} = 24$$

$$\%BKG = 24/27000 = 0.1\%$$

The amount of background due to $\psi' \to \pi^+\pi^- J/\psi, J/\psi \to \rho\pi$ events is negligible. In fact, the estimate is probably an overestimate, since potential $J/\psi \to l^+l^-$ events that Daniela vetoed were kept in the sample. This channel should be one of the largest contributors to hadronic background. There are many other channels, but most of them have either higher multiplicities or higher mass particles and will be killed even more effectively by our kinematic cuts. Therefore the hadronic background is expected to be small.

Monte Carlo

The Monte Carlo generator used is PPGEN. A total of 100,000 (153 realization) plus 177,000 (154 realization) Monte Carlo events are generated each for the $\psi' \to \pi^+\pi^- J/\psi$, $J/\psi \to e^+e^-$ and $\psi' \to \pi^+\pi^- J/\psi$, $J/\psi \to \mu^+\mu^-$ samples.

The Monte Carlo[6] assumes:

1. The orbital angular momentum between $\pi\pi$ system and J/ψ and between π's in the $\pi^+\pi^-$ system is 0.

2. The mass of the $\pi\pi$ system is weighted towards high mass.

$$\frac{d\sigma}{dm_{\pi\pi}} \propto \text{phase space} \times (M^2_{\pi\pi} - 4m^2_\pi)^2$$

3. Sequential 2-body decays: $\psi' \to X + J/\psi$, $X \to \pi^+\pi^-$, and $J/\psi \to l^+l^-$.

4. X and J/ψ are uniformly distributed.

5. π's are uniformly distributed in X rest frame.

6. Leptons have $1 + \cos^2\theta$ distribution in J/ψ rest frame.

7. J/ψ decay has α^3 order final state radiative correction in CMS of J/ψ.

Data - Monte Carlo Comparison.

Figs. 12-15 show a comparison of data and Monte Carlo for an assortment of plots. The agreement is good, in general, confirming that the cuts used eliminate background. However, the Monte Carlo does not fit m_{recoil} distribution well.

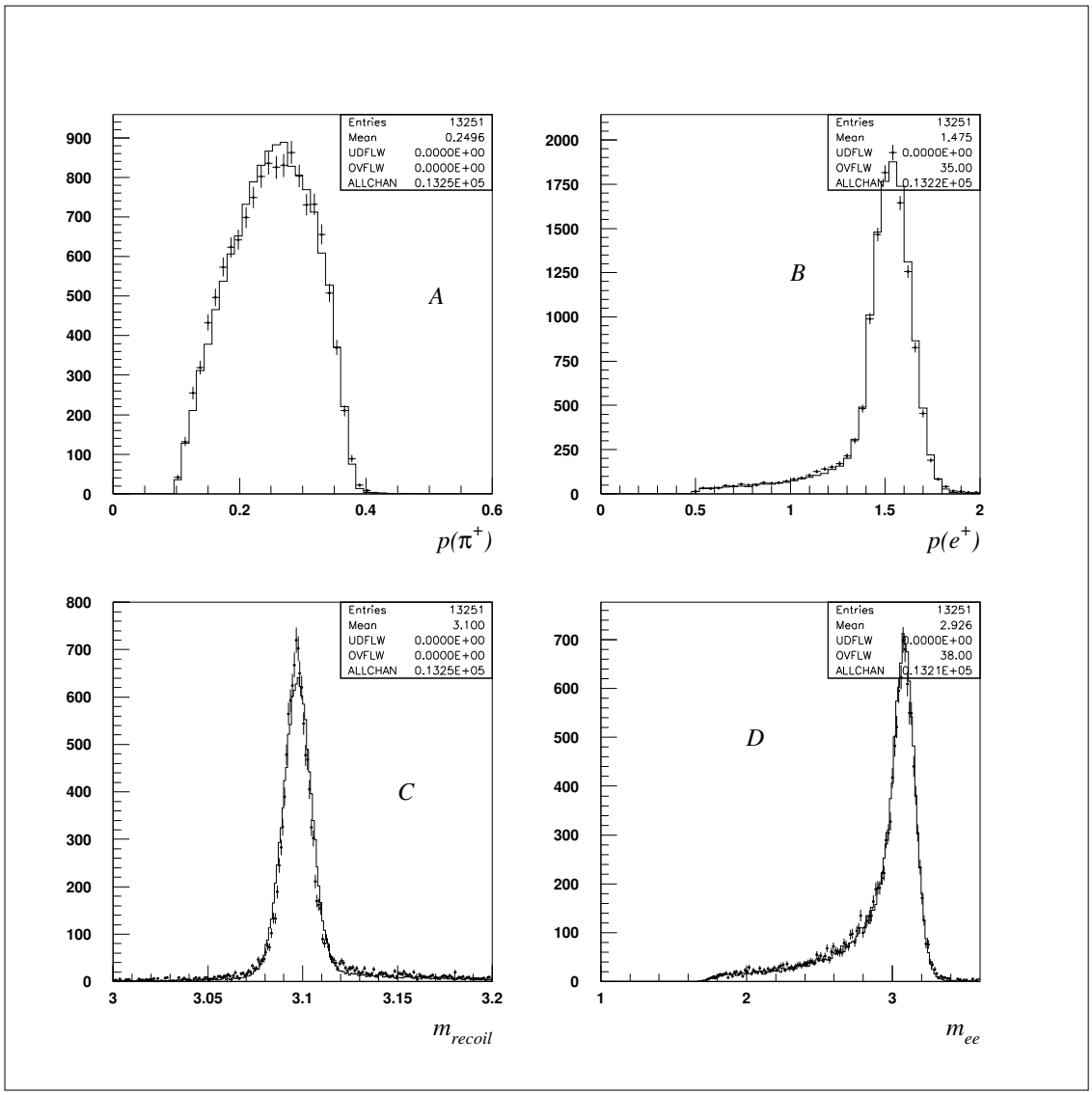

Figure 12: Comparison between $\psi' \to \pi^+\pi^- J/\psi$, $J/\psi \to e^+e^-$ data (dots with error bars) and Monte Carlo data (histogram). A.) p_{π^+}. B.) p_{e^+}. C.) m_{recoil}. D. $m_{e^+e^-}$.

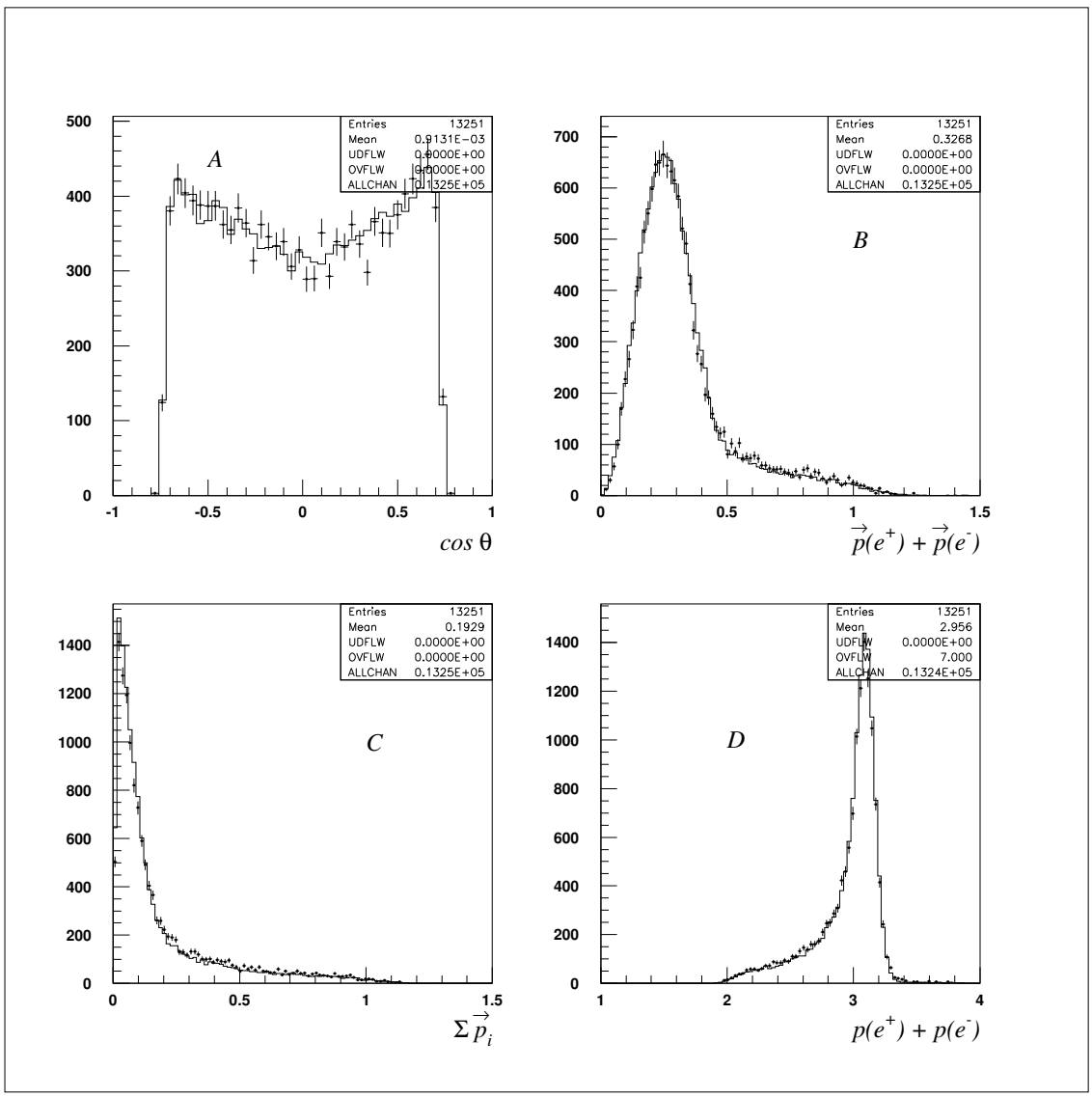

Figure 13: Comparison between $\psi' \to \pi^+\pi^- J/\psi$, $J/\psi \to e^+e^-$ data (dots with error bars) and Monte Carlo data (histogram). A.) $\cos\theta_e$ distribution. B.) $\vec{p}(e^+) + \vec{p}(e^-)$ distribution. C.) $\Sigma_{i=1}^{4}\vec{p}_i$ distribution. D. $p(e^+) + p(e^-)$ distribution.

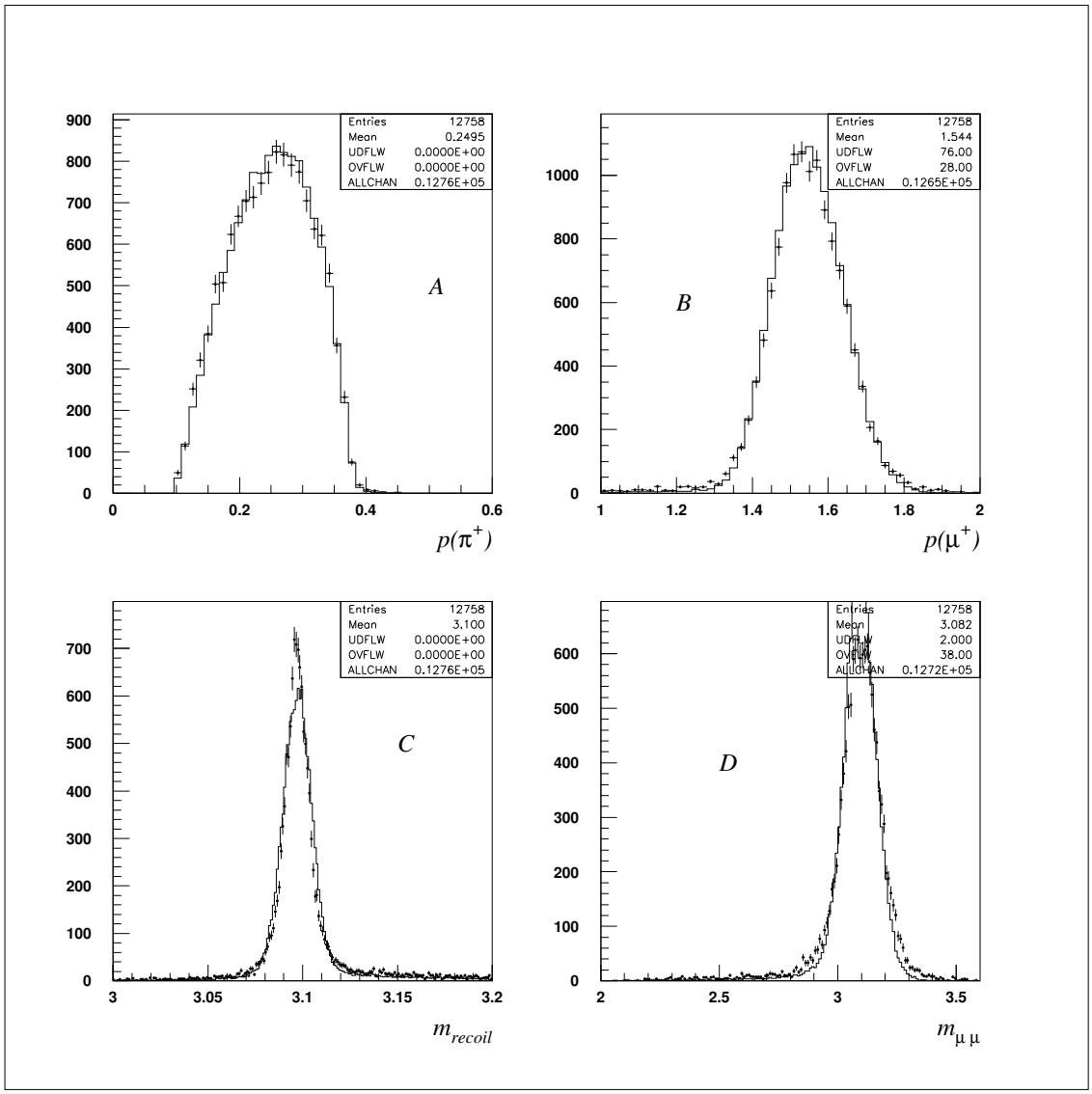

Figure 14: Comparison between $\psi^{'} \to \pi^+\pi^- J/\psi$, $J/\psi \to \mu^+\mu^-$ data (dots with error bars) and Monte Carlo data (histogram). A.) p_{π^+} B.) p_{μ^+} C.) m_{recoil} D. $m_{\mu^+\mu^-}$

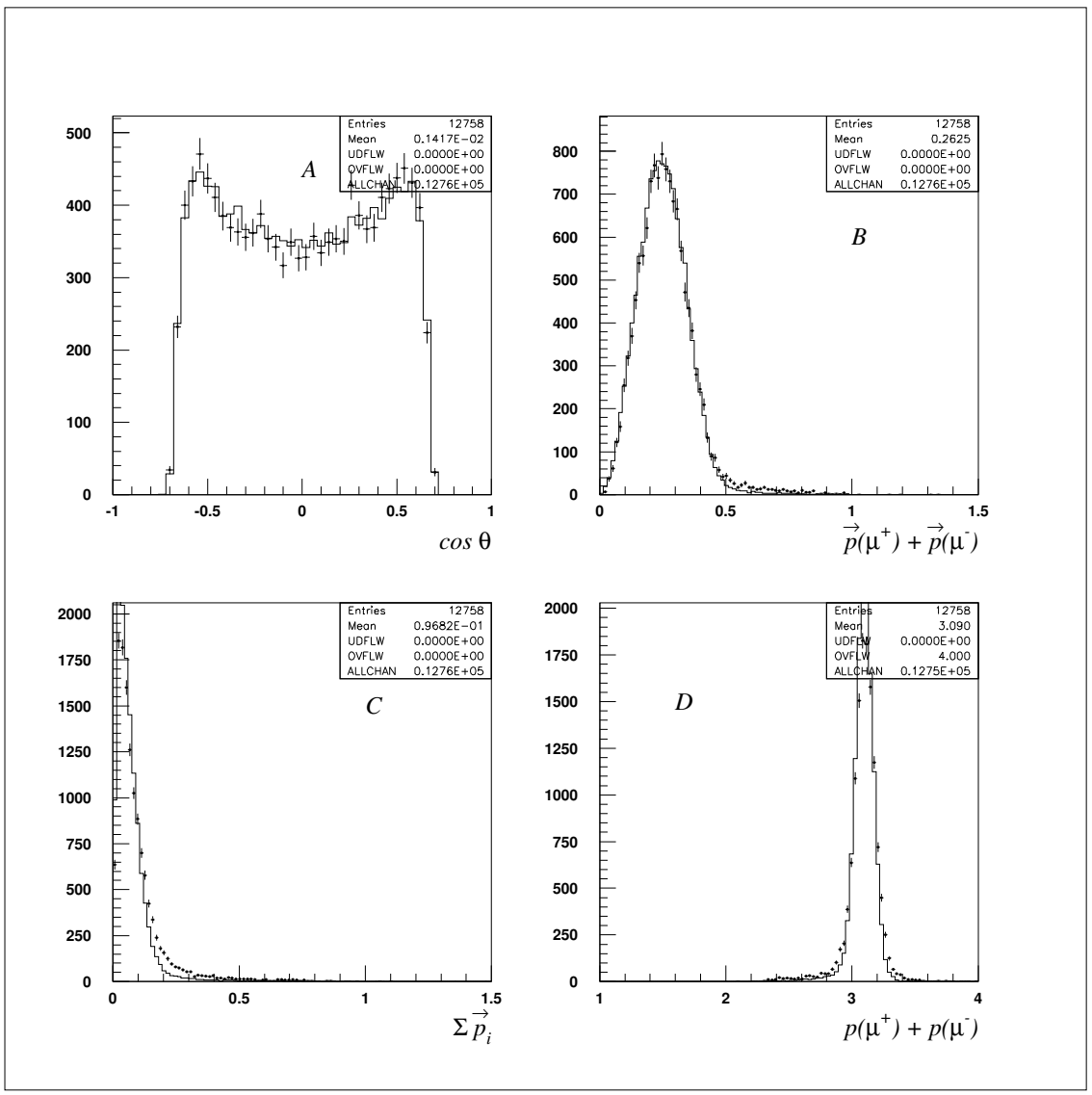

Figure 15: Comparison between $\psi' \to \pi^+\pi^- J/\psi$, $J/\psi \to \mu^+\mu^-$ data (dots with error bars) and Monte Carlo data (histogram). A.) $\cos\theta_\mu$ distribution. B.) $\vec{p}(\mu^+) + \vec{p}(\mu^-)$ distribution. C.) $\Sigma_{i=1}^{4}\vec{p}_i$ distribution. D. $p(\mu^+) + p(\mu^-)$ distribution.

Branching Ratio Results

The results are given in Table 5. NOTE: The small corrections for backgrounds and for data-Monte Carlo efficiency differences have not been put in. These differences will be included in the systematic errors.

Table 5: RESULTS.

Result	'93 Data	'95 Data
$N_{\mu\mu}$	7388	13738
N_{ee}	7386	13269
$N\psi'$	1.31×10^6	2.36×10^6
$B(ee)$	$(5.79 \pm 0.10)\%$	$(6.02 \pm 0.08)\%$
$B(\mu\mu)$	$(5.96 \pm 0.10)\%$	$(5.90 \pm 0.08)\%$

Combining:

$$BR(ee) = (5.933 \pm 0.061)\%$$

$$BR(\mu\mu) = (5.918 \pm 0.061)\%$$

$$BR(ll) = (5.926 \pm 0.043)\%$$

$$\chi^2 = 3.55$$

$$CL = 30\%$$

Study of Systematic Errors

In order to determine the systematic error, we have made many variations of our cuts. The results are given in Tables 6 and 7.

Table 6: Systematic Studies - '93 Data

Variation	$N_{\psi'}$	$N_{e^+e^-}$	$N_{\mu^+\mu^-}$	$B(e^+e^-)$	$B(\mu\mu)$
Standard (status > 0)	1308161	7388	7386	5.790	5.960
status > 1	1277374	7168	7205	5.753	5.954
3rd Order Background	1314680	7388	7385	5.761	5.930
$\cos\theta < .85$	1298695	8008	8014	5.782	5.947
$\cos\theta < .75$	1321826	6710	6716	5.777	5.973
mfit=2	1269193	6761	6836	5.703	5.924
$\chi_\pi < 2.5$	1290410	7154	7140	5.827	6.002
no π cuts ($pxy(\pi)$, $\Sigma Hit_\pi^{dE/dx}$,$\chi_\pi^{dE/dx}$)	1365882	8621	8497	5.796	5.879
rcmass ($2.95 < m < 3.25$)	1326154	7527	7519	5.760	5.928
$\lvert\cos\theta_\mu\rvert < 0.6$	1307539	7388	6908	5.792	5.953
no $\cos\theta_{l^+l^-}$ or $\cos\theta^{cm}_{l^+l^-}$ cut	1309852	7478	7455	5.807	5.976
Use (E/p) cut if p > 0.65 GeV/c	1307860	7377	7386	5.779	5.962
p_l^+ or p_l^- > 1.3 GeV/c	1307285	7579	7397	5.812	5.968

Table 7: Systematic Studies - '95 Data

Variation	$N_{\psi'}$	$N_{e^+e^-}$	$N_{\mu^+\mu^-}$	$B(e^+e^-)$	$B(\mu\mu)$
Standard (status > 0)	2361151	13738	13269	6.018	5.895
status > 1	2270682	13243	12922	6.033	5.969
3rd Order Background	2363765	13738	13269	6.011	5.889
$\cos\theta < .85$	2326046	14834	14273	6.044	5.886
$\cos\theta < .75$	2384883	12470	12043	5.979	5.877
mfit=2	2271991	12552	12193	5.978	5.851
$\chi_\pi < 2.5$	2336665	13298	12864	6.030	5.937
no π cuts ($pxy(\pi)$, $\Sigma Hit_\pi^{dE/dx}$,$\chi_\pi^{dE/dx}$)	2471424	15872	15236	5.993	5.797
rcmass ($2.95 < m < 3.25$)	2408771	13993	13526	5.947	5.835
$\lvert\cos\theta_\mu\rvert < 0.6$	2363415	13740	12431	6.013	5.886
no $\cos\theta_{l^+l^-}$ or $\cos\theta^{cm}_{l^+l^-}$ cut	2361502	13921	13404	6.047	5.923
Use (E/p) cut if p > 0.65 GeV/c	2361196	13742	13269	6.017	5.894
p_l^+ or p_l^- > 1.3 GeV/c	2361377	14093	13302	6.043	5.904

Final Results

Using the results from Tables 6 and 7 to determine the systematic errors, we obtain the results shown in Table 8.

Table 8: FINAL RESULTS.

Result	'93 Data (%)	'95 Data (%)
$B(ee)$	$5.79 \pm 0.10 \pm 0.12$	$6.02 \pm 0.08 \pm 0.13$
$B(\mu\mu)$	$5.96 \pm 0.10 \pm 0.12$	$5.90 \pm 0.08 \pm 0.16$

$$BR(ee) = (5.93 \pm 0.06 \pm 0.13)\%$$

$$BR(\mu\mu) = (5.92 \pm 0.06 \pm 0.14)\%$$

$$BR(ll) = (5.93 \pm 0.04 \pm 0.13)\%$$

References

[1] See: "Analysis Note: Number of ψ' Events", F. A. Harris, 5/1997.

[2] Bill Dunwoodie and Li Xinhua have studied the dE/dx TOF information for the ψ' data and have written routines to correct it.

[3] MnFit: Brock, I. C., L3 Note 918, June 1994. Here we shift and scale the Monte Carlo E/p distribution using:

$$(E/p)_{new} = scale * (E/p)_{old} + shift.$$

[4] OKSPI was written by Yuan Changzheng. It corrects for the shift observed and then uses 3 σ cuts in terms of the measured σ for each data set.

[5] MYMUID was written by Yuan Changzheng. It checks the track matches in the muon counters after making empirical shifts to the counters positions. My version corrects a mistake in this routine. I have also checked that I obtain the same results not using this routine and just using the muon bits directly.

[6] BES Collaboration, "Determination of the J/ψ Leptonic Branching Fraction via $\psi(2S) \to \pi^+\pi^- J/\psi$", draft of Oct. 94.